# 1

# Introduction

## 1.1 Background

When we are confronted by a problem, simple or complex, we tend to decompose it in order to achieve a solution. For instance, if the lights go out in our room, we first ask ourselves, if the switch is still on; if on, we next search for a fuse box and if unsuccessful, we proceed to question whether the actual power source is available. In more complex scenario, if our car stops unexpectedly while driving, we first check the fuel gauge, then the battery, and then search various components of the engine based on telltale sounds that may have occurred. These are problems that occur in everyday life and exemplify the concept of decomposition. Engineers and scientists "decompose" complex signal/system problems into separate components in order to comprehend their superposition or overall performance. Thus, the understanding of signal components or subsystems is necessary in order to analyze or modify complex signals or systems. In this text, we develop techniques that enable us to perform this decomposition in order to simplify the signal/system into more comprehensible components. For example, in chemistry, when presented with an unknown substance to be analyzed, a chemist will perform the analysis by applying mass spectrometry to decompose it into constituent components. In criminal forensics, investigators decompose the crime scene to determine the cause, weapons, to piece together a scenario that will lead to the identification of the perpetrators. In energy science, scientists decompose nuclear reactions into constituent components to achieve higher energy yields. Control/structural engineers intensely study second-order system performance that can be used to evaluate complex systems like motors or bridges or building responses based on decomposing them into these simpler subsystem responses. Given noisy, uncertain measurement data, signal processors perform routine spectral analysis to reveal constituent components in order to separate signals from the noise. Applications like extracting the pregnant mother's heart beats from those of the fetus are achieved by decomposition techniques. Complex



*Signal Processing: An Applied Decomposition Approach*, First Edition. James Vincent Candy.

Companion website: www.wiley.com/go/CandySignProc

detection problems can also be solved by techniques such as decentralized detector design by decomposing the problem into local detectors reporting to a central processor. All-in-all, the decomposition approach to problem-solving from the simple to the complex is routine, often going unnoticed, in everyday life as well as in sophisticated scientific engineering applications. This text presents "decomposition" from the signal/system perspective.

We must first decide on the essence of the signal itself. Is it deterministic or random? A *deterministic signal* is characterized by its repeatability, that is, it is free from variations and repeatable from measurement to measurement, while if it varies extraneously, then it is no longer repeatable and it is defined simply as a *random signal*. Here we are concerned with the development of processing techniques to extract the pertinent information from random signals using any a priori information available. These techniques are called *signal estimation* with enhancement achieved by applying a particular algorithm called a *signal estimator* or just *estimator* that is annotated by a "$\wedge$." We start with a simple example.

**Example 1.1** Suppose we are given sinusoidal data, $x(t_k)$, sampled at approximately 0.1 sec depicted in Figure 1.1a, and wish to decompose it by separating the signal, $s(t_k)$, from any disturbances, $d(t_k)$, and noise, $n(t_k)$.

$$x(t_k) = s(t_k) + d(t_k) + n(t_k) \tag{1.1}$$

That is, we would like to analyze its components that represent the desired signal to be extracted along with undesirable disturbances to be removed along with inherent measurement (numerical) noise. The first step a signal processor would pursue is to perform an analysis of the frequency spectrum as shown in Figure 1.1b. The signal is assumed to be deterministic (nonrandom) ignoring any uncertainties. Performing a discrete Fourier transform (*DFT*) on the data reveals spectral peaks corresponding to the sinusoids,

$$\mathcal{F}(\Omega_m) = \sum_{k=1}^{N} x(t_k) e^{-j\Omega_m t_k} \quad \text{for} \quad \Omega_m := \left(\frac{2\pi}{N}\right) \times m \tag{1.2}$$

It is clear from the spectrum that resonances exist at three temporal frequencies of 0.1225, 0.3228, and 0.496 Hz. If we were analytically aware (a priori) that the signal was composed of three sinusoids

$$s(t_k) = A_1 \cos(\omega_1 t_k + \phi_1) + A_2 \cos(\omega_2 t_k + \phi_2) + A_3 \cos(\omega_3 t_k + \phi_3) \quad \text{for} \quad \omega := 2\pi f \tag{1.3}$$

the sinusoidal transform relation assuming zero phases ($\phi_k \approx 0$) is given by

$$S(\omega) = \sum_{k=1}^{3} A_k \left[\delta(\omega - \omega_k) + \delta(\omega + \omega_k)\right] \quad \text{for} \quad \omega_k := 2\pi f_k \tag{1.4}$$

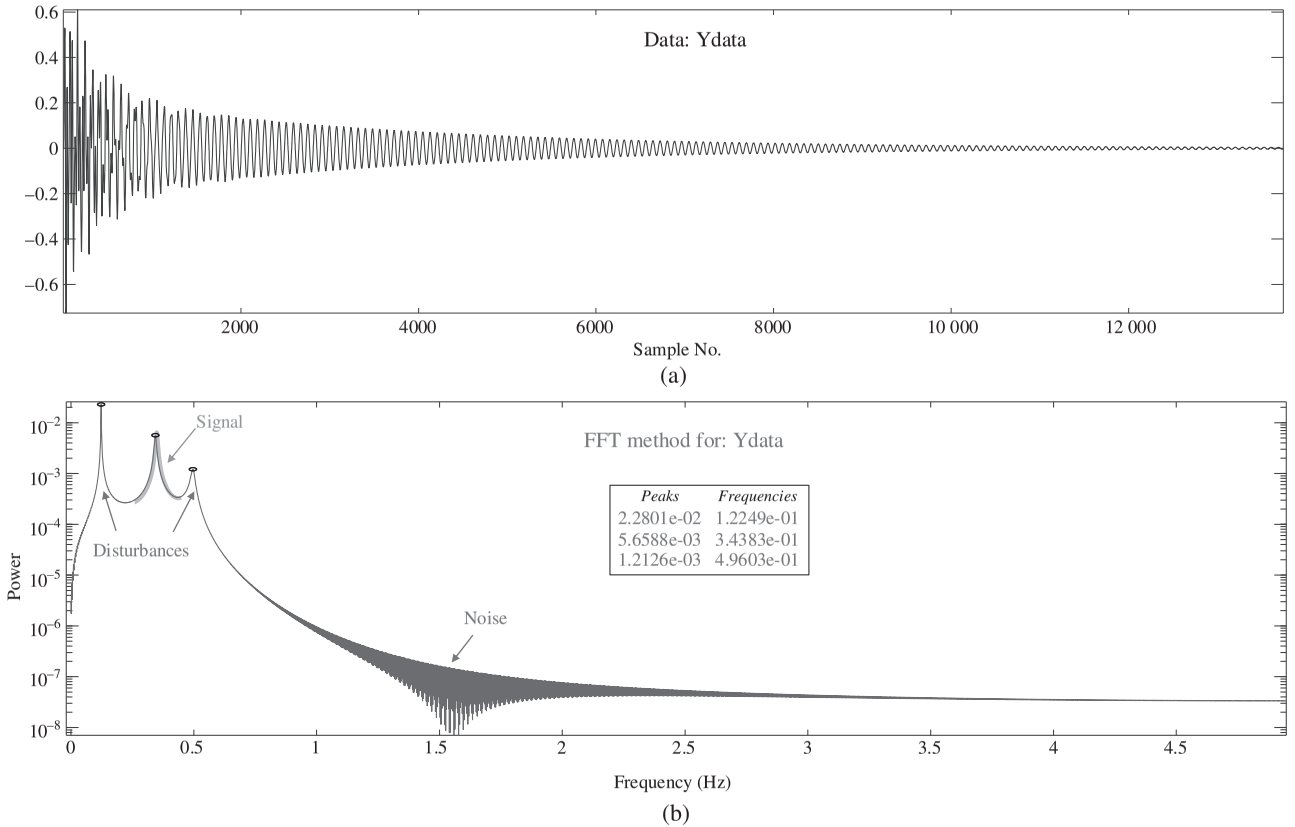


**Figure 1.1** *Deterministic* sinusoidal data: (a) composite signal consisting of three sinusoids at frequencies of 0.1225, 0.3228, and 0.496 Hz, zero phase at a large *SNR* (200 dB). (b) Composite Fourier spectrum illustrating three sinusoidal peaks consisting of two disturbances and the actual signal (thick line) along with numerical noise.

and we expect to observe perfect spectral lines (impulses) located at these specified frequencies. However, since there is leakage in the discrete Fourier spectral estimation created by truncating the data abruptly, a small DC-component appears creating a smearing of the peaks that result in a spectral width yet still providing correct peak frequencies. So we see ideally that the Fourier transform decomposes the composite signal of superposed sinusoids into the three spectral peaks enabling us to analyze its composition and consider separating them into its constituent components.

△△△

Next, the signal processor may know (a priori) from the underlying physics of the problem that generated this data that the actual signal is located between 0.15 and 0.4 Hz, while a pair of disturbances, $d(t_k)$ caused by local signals lie outside that band, that is,

$$0.15\,\text{Hz} < s(t_k) < 0.40\,\text{Hz} \quad \text{and} \quad 0.15\,\text{Hz} > d(t_k) \quad \text{or} \quad d(t_k) > 0.4\,\text{Hz}$$

**Example 1.2** Consider the same sinusoidal data of Example 1.1 contaminated by instrumentation noise and disturbances at a 0 dB signal-to-noise ratio (*SNR*). The noisy data and corresponding spectrum are shown in Figure 1.2a,b. Clearly from the figure, the corresponding spectral (Fourier) data still indicate the presence of three sinusoidal peaks as before; however, the measurement instrumentation noise has distorted their locations somewhat at frequencies of 0.1219, 0.3450, and 0.4960 Hz instead of the true frequencies.

△△△

## 1.2 Spectral Decomposition

Simply treating these data as stochastic requires an improved spectral estimator to extract the peaks leading to the basis of power spectral density (*PSD*) estimation rather than simple Fourier (*FFT*) spectra. Perhaps the simplest spectral estimator follows by treating the data as a random signal. Techniques similar to deterministic theory hold when the random signal is transformed to its *correlation sequence* and its Fourier spectrum is transformed to its *power spectrum*. We know that the correlation sequence and power spectrum form a *DFT* pair, analogous to a deterministic signal and its corresponding spectrum, that is, we have that

$$\text{Fourier Transform}: \qquad R_{xx}(k) \longleftrightarrow S_{xx}(\Omega)$$

and as in the deterministic case, we can analyze the spectral content of a random signal by investigating its power spectrum. The *PSD* function for a discrete random process, $x(t_k)$ is defined as:

$$S_{xx}(\Omega) := \lim_{N\to\infty} E\left\{\frac{X(\Omega)X^*(\Omega)}{2N+1}\right\} \tag{1.5}$$

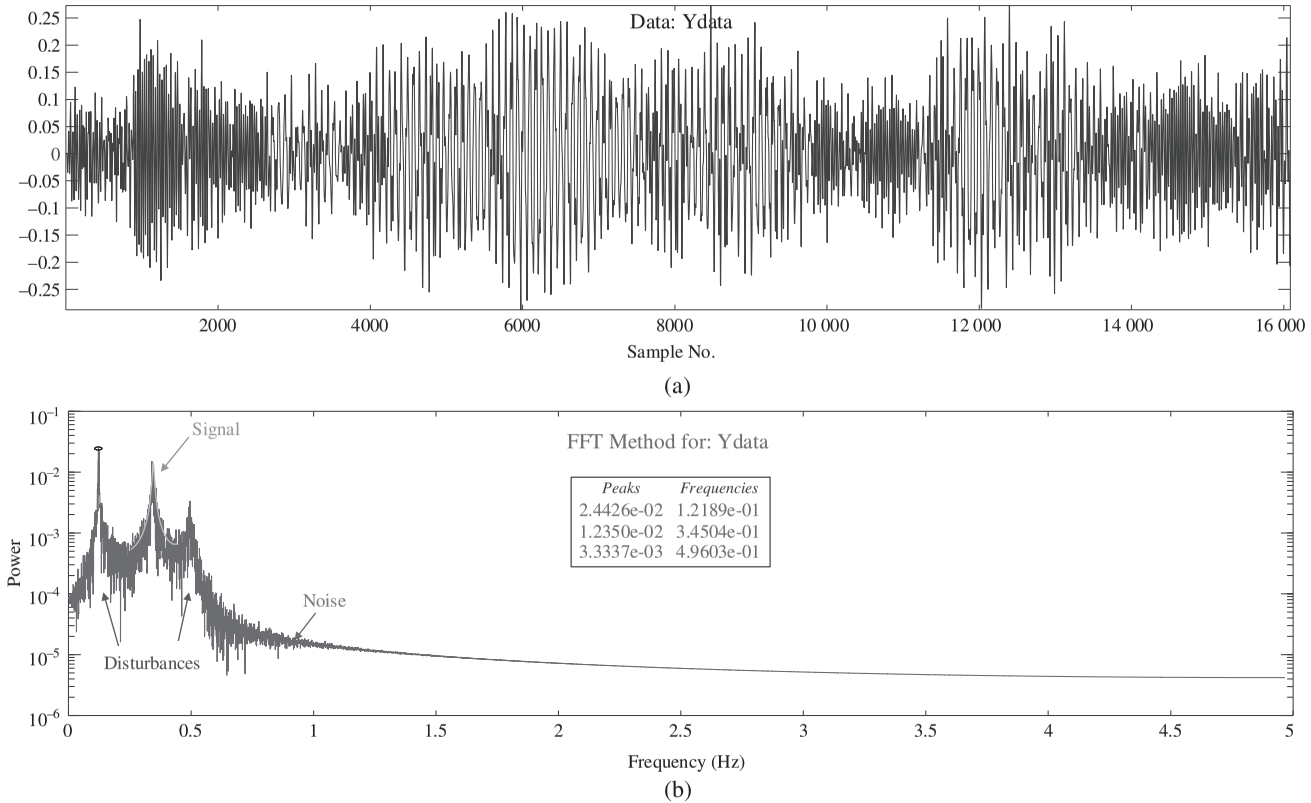


**Figure 1.2** *Random* sinusoidal data with disturbances and noise: (a) Composite signal consisting of three sinusoids at frequencies of 0.1225, 0.3228, and 0.4960 Hz. (b) Composite Fourier spectrum illustrating three noisy sinusoidal peaks at frequencies of 0.1219, 0.3450, and 0.4960 Hz consisting of two disturbances and the actual signal (thick line) along with numerical noise.

where $^*$ is the complex conjugate. The expected value operation $E\{.\}$ can be thought of as "mitigating" the randomness. Similarly, the *correlation* (at lag $k$) is

$$R_{xx}(k) := E\{x(t)x(t+k)\} \tag{1.6}$$

Recall that the *DFT pair* is defined by

$$X(\Omega_m) := \text{DFT}[x(t)] = \sum_{t=0}^{M-1} x(t)e^{-j\Omega_m t}$$

$$x(t) = \text{IDFT}\left[X(\Omega_m)\right] = \frac{1}{M}\sum_{t=0}^{M-1} X(\Omega_m)e^{j\Omega_m t} \tag{1.7}$$

for $\Omega_m = \left(\frac{2\pi}{M}\right)m$.

Therefore, for $x(t_k)$, a random signal, we have that the correlation-power spectrum pair is (*Wiener–Khintchine theorem* [1])

$$\hat{S}_{xx}(\Omega_m) = DFT\left[\hat{R}_{xx}(k)\right]$$
$$\hat{R}_{xx}(k) = IDFT\left[\hat{S}_{xx}(\Omega_m)\right] \tag{1.8}$$

With the a priori information available about the signal and disturbance spectra, it is possible for the signal processor to perform a simple extraction by applying bandpass filters illustrating how the uncertain composite signal can be decomposed into its constituent components as previously performed by the Fourier decomposition (*DFT*) of the deterministic sinusoidal data of Figure 1.1. We illustrate this application in the following example.

**Example 1.3** Consider the noisy composite data of Example 1.2 with measurements acquired at a 0 dB *SNR* shown in Figure 1.2a. Bandpass filters are designed by the processor to extract the desired signal at 0.345 Hz rejecting disturbances at 0.1225 and 0.4960 Hz. The 256-weight finite impulse response (*FIR*) filters are designed to operate within the respective frequency bands of (0.025–0.15) Hz, (0.2–0.4) Hz, and (0.4–0.5) Hz. The results are shown in Figure 1.3 for each band. △△△

This example illustrates the fundamental concepts of decomposing a composite noisy measurement into its constituent components using any a priori information to perform a simple decomposition and extraction of the desired signal. Next, we consider more sophisticated methods of achieving such a decomposition.

## 1.3 Data Decomposition

Data are acquired in a variety of domains depending on the particular application and hardware available. In this text, we will consider the usual time domain

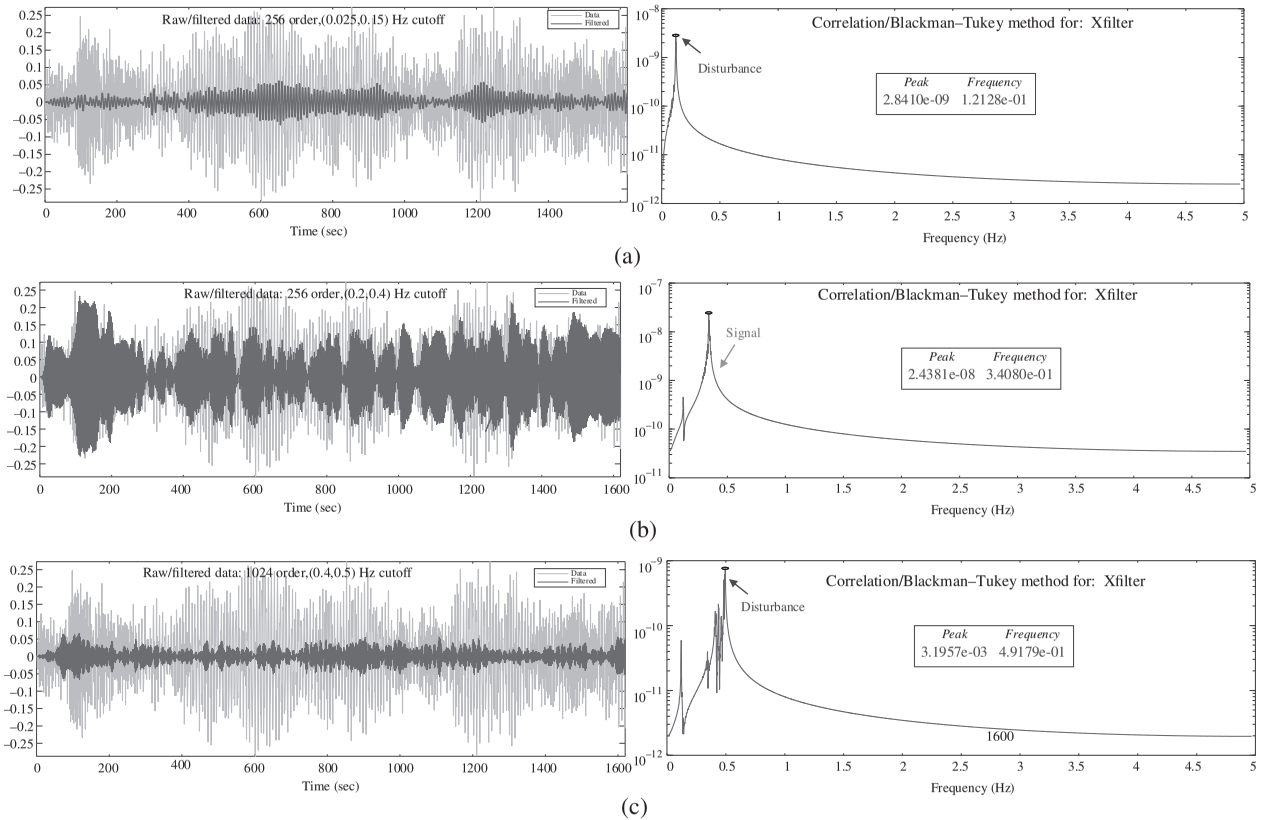


**Figure 1.3** Filtering *random* sinusoidal data for decomposition/extraction: (a) Disturbance at 0.1225 Hz separation using (0.025, 0.15) Hz bandpass filter: signal and power spectrum. (b) Signal at 0.3450 Hz extraction using (0.2, 0.4) Hz bandpass filter: signal and power spectrum. (c) Disturbance at 0.4960 Hz separation using (0.4, 0.5) Hz bandpass filter: signal and power spectrum.

data (time series), frequency domain data (spectra) along with space–time (spatiotemporal) or space–frequency (frequency–wavenumber) data sets. Once data, either single or multichannel, are acquired, it can be arranged in a variety of data structures for processing. The most common arrangement is the vector-matrix structure, that is, the data can be placed into a so-called data matrix and processed accordingly. Data decomposition methods follow based on the underlying nature of the problem and the domain selected. For instance, vibration responses are usually measured in the time domain using multichannel tri-axial (vector) accelerometers leading to the data matrix, while in a nondestructive evaluation application such as resonant ultrasound, frequency domain data are acquired leading to a complex frequency data matrix for subsequent processing. It is the underlying internal structure of the data matrix that leads to a particular decomposition technique.

For our previous sinusoidal problem, we showed how spectral decomposition and processing (bandpass filtering) led to a simple decomposition and signal extraction technique that is easily applied to analyze and process the noisy time series data. These data can then be transformed directly to the frequency domain or have been measured directly in that domain and arranged in a particular structural matrix for decomposition.

With this in mind, we can define a sequence of time domain data by a set of $N_t$-samples, $\{x(t)\}; t = 0, 1, \ldots, N_t - 1$ for $t$ the discrete-time index. Therefore, this sequence can be considered an $N_t$-vector such that $\mathbf{x}(t) \in \mathcal{R}^{N_t \times 1}$. Similarly, the set of frequency domain data $\{X(\omega_k)\}; k = 0, 1, \ldots, N_\omega - 1$ for $\omega_k$, the discrete frequency can be defined by the complex $N_\omega$-vector, with $\mathbf{X}(\omega_k) \in C^{N_\omega \times 1}$. Spatiotemporal or spatio-frequency data also follow as $\mathbf{x}(t, z)$ and $\mathbf{X}(\omega, \kappa)$ with $z$, the spatial variable, and $\kappa$, the spatial frequency or wavenumber. In any case with the "data vector" defined, a variety of data matrices can be constructed. For instance, if $x(t)$ represents the deterministic impulse response of a system, then the corresponding frequency response vector or transfer function is simply its Fourier transform, that is,

$$\mathbf{x}(t) \Longrightarrow \mathcal{F}(x(t)) \Longrightarrow \mathbf{X}(\omega_k)$$

However, if the data are considered random, then its correlation function is estimated leading to the correlation matrix

$$\mathbf{x}(t) \Longrightarrow E\{\mathbf{x}(t)\mathbf{x}^\dagger(t)\} \Longrightarrow \mathbf{R}_{xx}$$

with corresponding power spectral matrix evolving as

$$\mathbf{X}(\omega) \Longrightarrow E\{\mathbf{X}(\omega)\mathbf{X}^\dagger(\omega)\} \Longrightarrow \mathbf{S}_{xx}(\omega)$$

So we see that the vector-matrix representation of a signal is a common representation in statistical signal processing leading to a wide expanse of techniques and decompositions based on the internal structure of the constructed data matrix.

For example, in realization theory impulse response data are constructed in a Hankel matrix that possesses critical system theoretical properties, while in linear prediction theory data are constructed in Toeplitz matrices dominating algorithm developments [1, 2]. In fact, we note in passing that the important data matrices constructed in signal processing are typically the impulse response matrix, $\mathbf{H}$, the correlation matrix, $\mathbf{R}_{xx}$, the frequency response or transfer function matrix, $\mathbf{F}$—all of which are easily decomposed using numerical factorization methods such as Cholesky decomposition, LU-decomposition, eigen-decompositions, and singular value decompositions [3]. For example,

$$\mathbf{H} = \mathbf{LU}; \quad \mathbf{R}_{xx} = \mathbf{U}\Lambda\mathbf{U}^{\dagger}; \quad \mathbf{F} = \mathbf{U}'\mathbf{V}^{\dagger}; \quad \mathbf{S}_{xx} = \mathbf{LDL}^{\dagger}$$

It is these types of decomposition approaches that will be developed throughout this text. Let us return to our sinusoidal example and apply the decomposition approach to illustrate this concept [4, 5].

**Example 1.4** Consider the same sinusoidal data of Example 1.1 contaminated by instrumentation noise and disturbances at a 0 dB *SNR*. The noisy data are shown in Figure 1.4a. First, the $N_t$-data vector $\mathbf{x}(t)$ is used to estimate the correlation matrix, $\mathbf{R}_{xx}$. Next, this matrix is processed by performing an eigen-decomposition such that

$$\mathbf{R}_{xx} = \mathbf{E} \times \Lambda \times \mathbf{E}^{\dagger}$$

From this decomposition, a subset of the eigenvectors, $\{\mathbf{e}_i\}; i = 1, \ldots, N_s$, are selected and a corresponding power estimator created such that

$$P(\omega) = \frac{1}{\sum_{i=N_s+1}^{N_t} |\mathbf{v}^{\dagger}(\omega)\mathbf{e}_i|}$$

where $\mathbf{v}(\omega) = [1 \; e^{-j\omega} \; e^{-j2\omega} \; \cdots \; e^{-j(N_t-1)\omega}]'$ is a complex vector of discrete frequencies. Applying this decomposition processor to the reduced correlation data results in the spectrum shown in Figure 1.4b. The spectrum is very smooth and results in reasonable frequency (peak) estimates at frequencies of 0.1231, 0.3444, and 0.4973 Hz as annotated in the figure. The power estimator is the 24th-order multiple signal classification (*MUSIC*) harmonic estimation algorithm completing the example and illustrating a data decomposition approach [6].

△△△

Spatiotemporal (space–time) data or wave phenomena occur in a wide variety of applications ranging from the simple dropping of a pebble into a puddle generating spherical waves; to ocean acoustic wave propagation searching for unknown targets; to tracking aircraft/missiles during conflicts; to locating flaws in materials [1, 7–9]. Typically, the problem is to separate or decompose sources or scatterers for analysis, whether they are benign or malignant tumors or friendly/unfriendly

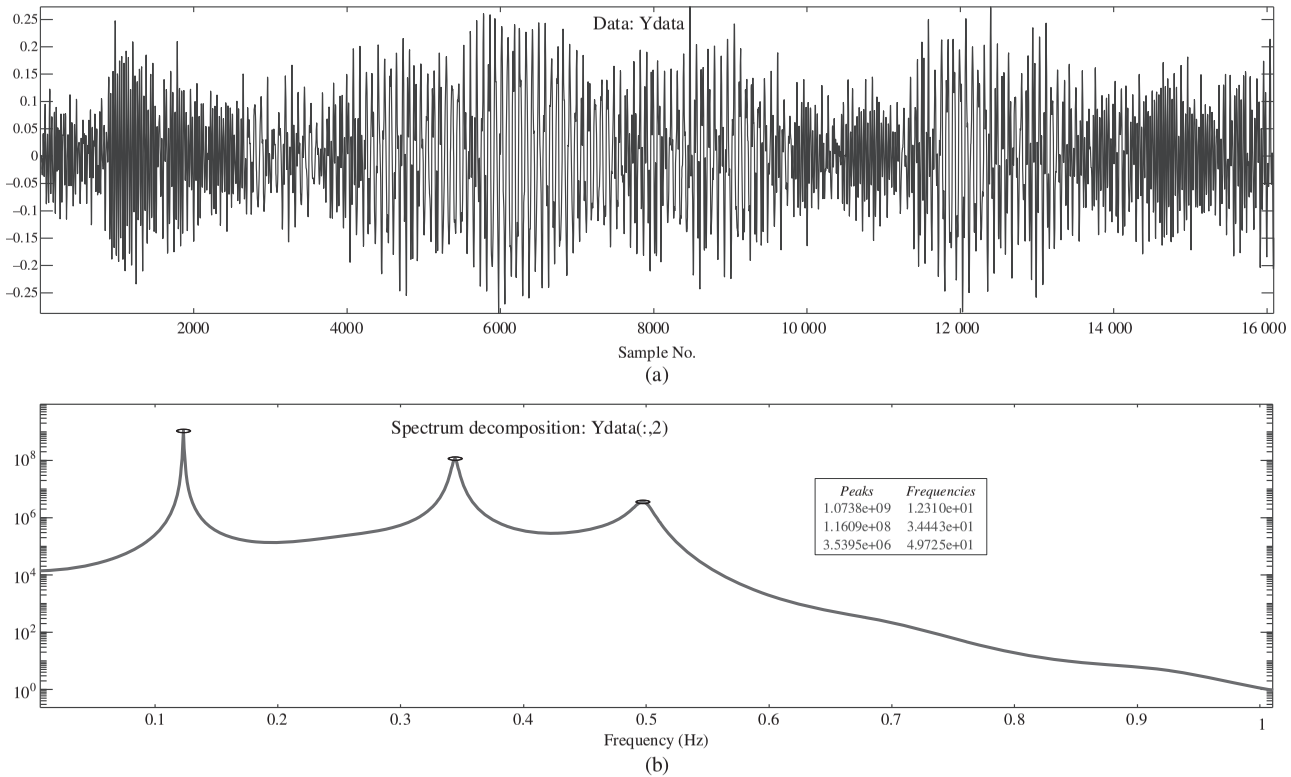


**Figure 1.4** Spectral decomposition of noisy (0 dB) sinusoidal data: (a) Composite signal consisting of three sinusoids at frequencies of 0.1225, 0.3228, and 0.4960 Hz. (b) Decomposed power spectrum (*MUSIC*: Order = 24) with three noisy estimated peaks at frequencies of 0.1231, 0.3444, and 0.4973 Hz.

targets [8, 9]. In any case, the goal remains the same—the decomposition of the space-time waves into individual scattering components. The following example illustrates how spatiotemporal processing can achieve such a decomposition.

A narrowband, *spatiotemporal wave signal* can be defined by an $L$-element sensor array measurement model contaminated by random noise as [8]

$$\mathbf{y}(t) = D(\kappa)\mathbf{s}(t) + \eta(t) \tag{1.9}$$

where $\mathbf{y}, \eta \in C^{L\times 1}$ are the array measurement and noise vectors, $\mathbf{s} \in C^{N_s\times 1}$ is the signal vector and $D \in C^{L\times N_s}$ direction matrix that can be defined uniquely for planar or spherical wavefronts, and $\kappa_m$ the corresponding spatial frequency or wavenumber ($\kappa_o = \frac{\omega_o}{c} = \frac{2\pi}{\lambda_o}$) for $c$ the propagation speed.

The wavenumber is a vector specifying the direction-of-arrival (*DOA*) of a wavefront as it impinges on the multichannel measurement array at an angle of incidence, $\theta_o$, which the direction vector makes with the array vertical reference, defined in terms of the wavenumber and sensor locations.

For instance, a harmonic plane wave signal vector can be represented by

$$\mathbf{s}(\mathbf{r};t) = \alpha_o e^{j\omega_o t}e^{-j\kappa_o\cdot\mathbf{r}} = \alpha_o e^{j\omega_o t}e^{-j(\kappa_x x+\kappa_y y)} = \alpha_o e^{j\left(\omega_o t-(|\kappa_o|\sin\theta_o x+|\kappa_o|\cos\theta_o y)\right)} \tag{1.10}$$

Therefore, the complex wavenumber vector has magnitude, $|\kappa| = \sqrt{\kappa_x^2+\kappa_y^2}$, and the angle is $\angle\kappa_{\mathbf{o}} = [\sin\theta_o \;\; \cos\theta_o]$. We see that in this case the plane wave is characterized by the parameter vector, $\Theta_o = \{\alpha_o, \kappa_o\}$ or equivalently $\Theta_o = \{\alpha_o, \omega_o, \theta_o\}$.

Consider the following example demonstrating the spatial–temporal method of decomposing noisy multichannel time series measurements in the spatial (Fourier) domain to extract independent source locations (bearing angles)—a common problem in sonar signal processing [9].

**Example 1.5** Suppose a 16-element, uniformly spaced at 2.5 m, linear array is impinged upon by a planar wavefront generated from three sources ($N_s = 3$) emanating from 20°, 40°, and 55° incidence angles. The temporal frequency is $\omega_o = 300$ Hz with corresponding propagation speed of $c = 1500$ m/sec. The sensor data are generated at 0 dB *SNR* and shown in Figure 1.5a. The order or number of sources is estimated using the information-theoretic techniques giving an $\hat{N}_s = 3$ with the corresponding plots shown in Figure 1.5b. The results of applying the power estimators are shown in Figure 1.5a,b, where we observe the ensemble results of the 16 sensor channels and the corresponding median spectral estimates. The results demonstrate that the algorithms are capable of decomposing the spatial spectrum providing reasonable *DOA* estimates. This completes the example.

△△△

So we see that the power spectral estimation techniques developed for temporal harmonic model-based parametric estimation map over to the wave type problems

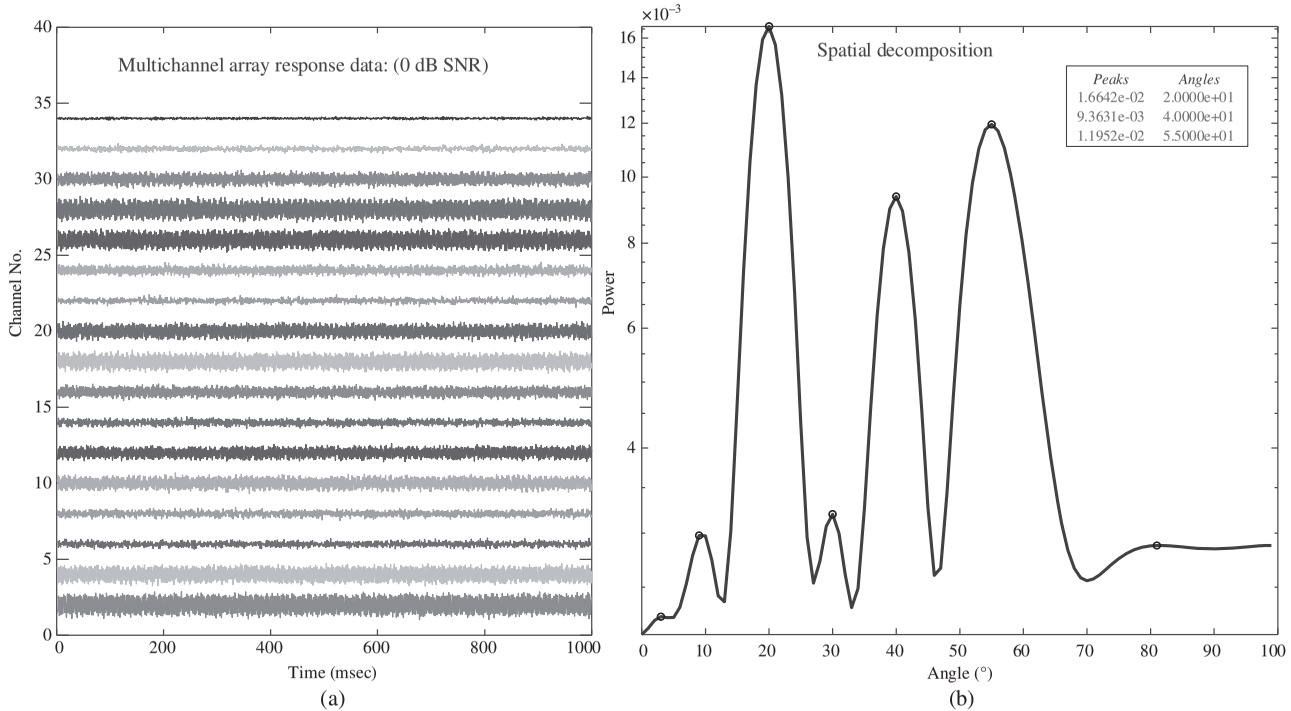


**Figure 1.5** Spatial spectral decomposition of multiple source data: (a) Multichannel array measurements (0 dB *SNR*). (b) Spectral source decomposition (degrees).

directly with the temporal harmonic signal vectors replaced by the spatial signal direction vectors.

Thus, we see how various data matrices can be simply decomposed using linear algebraic techniques applied to vectors/matrices of a specific data matrix. Next, we consider the model-based approach to perform signal/system decompositions.

## 1.4 Model-based Decomposition

Signal processing relies on any a priori knowledge of the phenomenology generating the underlying measurements. Characterizing this phenomenology and propagation physics along with the accompanying measurement instrumentation and noise are the preliminaries that must be tackled to solve a complex processing problem. In many cases, this is much easier said than done. The first step is to determine what the desired information is. In our case, we assume that the investigation is to extract information stemming from signals either emanating from a source whether it be an autonomous unmanned vehicle (*AUV*) passively operating in the deep ocean or a vibrating structure responding to ground motion. Applications can be very complex especially in the case of ultrasound propagating through complex media such as tissue in biomedical applications or through heterogeneous materials of critical parts in nondestructive evaluation (*NDE*) investigations [1, 10]. In any case, the processing usually involves manipulating the measured data to extract the desired information, such as location and tracking of the *AUV*, to failure detection for the structure, or tumor/flaw detection and localization in both biomedical and *NDE* [1, 5, 10].

Another view of the same problem is to decompose it into a set of steps that capture the strategic essence of the processing scheme. Inherently, the more a priori knowledge about the measurement and its underlying phenomenology that can incorporated into the processor, the better we can expect it to perform as long as the information that is included is correct. One strategy, called the "model-based approach," provides the essence of model-based signal processing (*MBSP*) [1, 10, 11]. Some believe that all of the signal processing schemes can be cast into this generic framework. Simply, the model-based approach is "incorporating mathematical models of both physical phenomenology and the measurement process (including noise) into the processor to extract the desired information." This approach provides a mechanism to incorporate knowledge of the underlying physics or dynamics in the form of mathematical propagation models along with measurement system models and accompanying uncertainties such as disturbances, instrumentation noise, or ambient noise as well as model uncertainties directly into the resulting processor. In this way, the signal processor enables the interpretation of results directly in terms of the underlying problem physics.

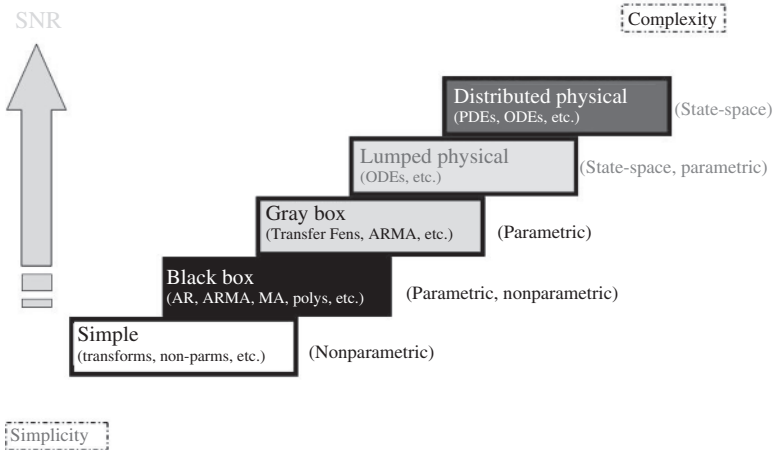


**Figure 1.6** Signal processing approach: the model-based "staircase." [Step 1] "Simple" nonparametric implicit models. [Step 2] "Black-box" models (transfer function, autoregressive, moving average, polynomial, etc.). [Step 3] "Gray-box" models (transfer function, moving average, etc.). [Step 4] "Lumped" physical ordinary differential equation models (state-space, parametric, etc.). [Step 5] "Distributed" physical partial differential equation models (state-space, etc.).

The model-based processor is really a modeler's tool enabling the incorporation of any a priori information about the particular application problem to extract the desired information. As illustrated in Figure 1.6, the fidelity of the incorporated model determines the complexity of the processor. These models can range from simple implied nonphysical representations of the measurement data such as the Fourier or wavelet transforms to parametric black-box models used for data prediction, to lumped mathematical physical representations characterized by ordinary differential equations, and to full physical partial differential equation models from finite element models capturing the critical details of propagation physics in a complex medium. The dominating factor of which model is the most appropriate is usually determined by how severe the measurements are contaminated with noise and the underlying uncertainties encompassing the philosophy of "letting the problem dictate the approach." If the *SNR* of the measurements is high, then simple nonphysical techniques can be used to extract the desired information. This approach of selecting the appropriate model is illustrated in the signal processing staircase of Figure 1.6 where we note that as we progress up the "modeling" steps to increase the *SNR*, the complexity of the model increases to achieve the desired results. In the following, we will apply the model-based framework to develop decomposition techniques for signal data as well as system models. This is our roadmap [10].

**Example 1.6** Suppose we have a noisy acoustical measurement of a single oscillation frequency contaminated by random noise at a 0 dB *SNR* and we would like to extract the desired information (the single oscillation frequency) as shown in Figure 1.7a. The "simple" approach to analyze the measurement data would be to take its Fourier transform and investigate the various frequency bands for resonant peaks. The result is shown in Figure 1.7b, where we observe a noisy spectrum and a set of potential resonances but nothing really conclusive. Next, we apply a broadband power spectral estimator with the resulting spectrum shown in Figure 1.7c. Here we note that the resonances have clearly been enhanced and appear in well-defined bands while the noise is attenuated by the processor, but there still remains a significant amount of uncertainty in the spectrum due to all of the resulting spectral peaks. Upon seeing these resonances in the power spectrum,

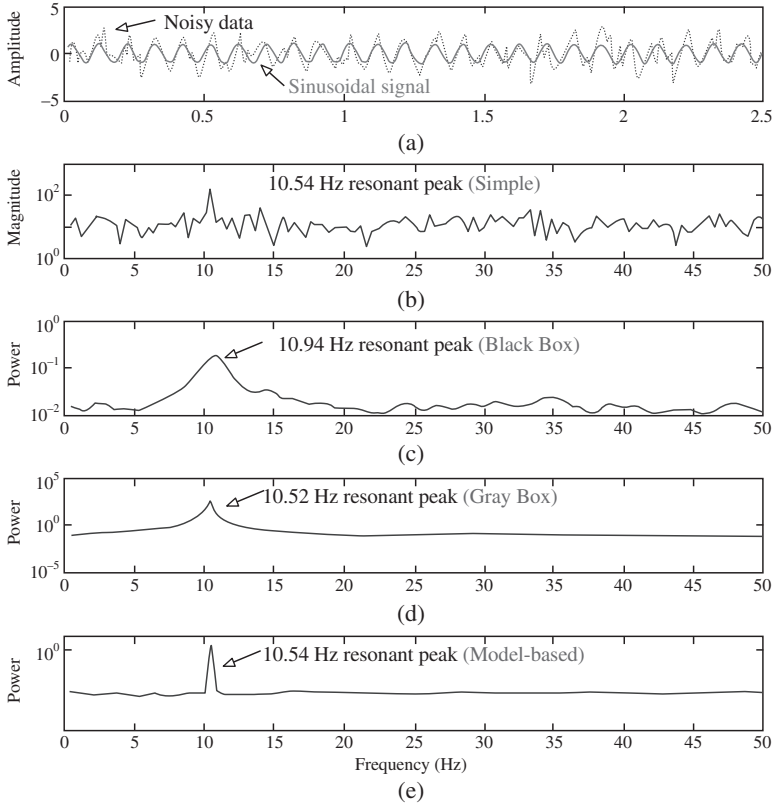


**Figure 1.7** Simple oscillation example. (a) Noisy oscillation (10.54 Hz) in noise. (b) Raw Fourier spectrum. (c) Nonparametric spectrum (black-box). (d) Parametric spectrum (gray-box). (e) Model-based spectrum (ordinary differential equation model).

we might proceed next to a gray-box model to enhance the resonances even further by using our a priori knowledge that there is essentially one dominant resonance. The results of applying this processor are shown in Figure 1.7d. Finally, we use this extracted model to develop an explicit model-based processor (*MBP*) by developing a set of harmonic equations for a sinusoid in noise and construct the *MBP* based on these relations. The results are shown in Figure 1.7e. So we see that once we have defined the processing problem, assessed the a priori information including the underlying phenomenology, then we can proceed up the staircase and exit any time we are satisfied with the result [1, 10].

△△△

It is important to investigate what, if anything, can be gained by processing the data. The amount of information available in the data is related to the precision (variance) of the particular measurement instrumentation used as well as any signal processing employed to enhance the outputs. As we utilize more and more information about generating the given data, we expect to improve our estimates (decrease estimation error) significantly.

A typical measurement $y$ is depicted in Figure 1.8 where we see the noisy measurement data and corresponding "final" estimates of the true signal bounded by its corresponding confidence intervals [12]. As we develop more and more sophisticated processors by including a priori knowledge in the algorithm, the

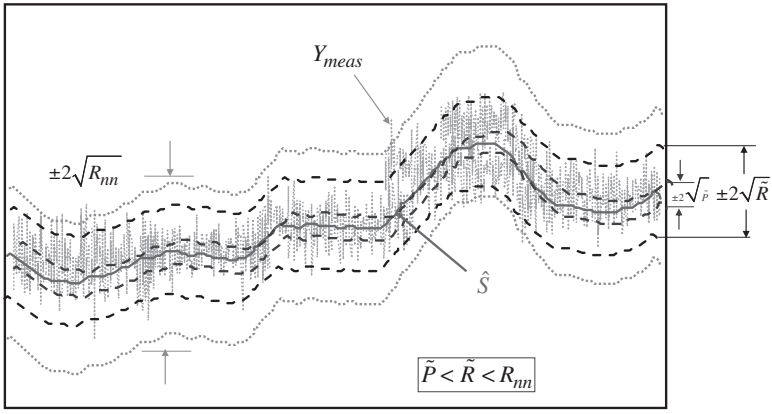


"the more a- priori information about the signal we can incorporate into the processor, the higher the precision (smaller error variance) we can achieve in estimation"

**Figure 1.8** Model-based signal processing of a noisy measurement conceptually illustrating that the more "a priori" information incorporated into the processor enables a reduction of the error variance.

uncertainty in the estimate decreases further as shown by the dashed bounds. Mathematically, we illustrate these ideas by the following.

In Figure 1.9a, the ideal measurement instrument is given by

$$Y_{meas} = S_{true} + N_{noise} \quad \text{[Ideal Measurement]}$$

and along with and a more realistic model of the measurement process is depicted in Figure 1.9b.

If we were to use $Y$ to estimate $S_{true}$ (that is, $\hat{S}$), we have the noise lying within the $\pm 2\sqrt{\tilde{R}}$ confidence limits superimposed on the signal (see Figure 1.8). The best estimate of $S_{true}$ we can hope for is only within the accuracy (bias) and precision (variance) of the instrument. If we include a model of the measurement instrument (see Figure 1.9b) as well as its associated uncertainties, then we can improve the SNR of the noisy measurements. This technique represents the processing based on our instrument and noise (statistical) models given by

$$Y_{meas} = C(S_{true}) + N_{noise}, \quad N \sim \mathcal{N}(0, R_{nn}) \quad \text{[Measurement and Noise]}$$

where $C(S_{true})$ is the measurement system model and $\mathcal{N}(0, R_{nn})$ is the noise statistics captured by a *Gaussian* or *normal distribution* of zero-mean and variance specified by $R_{nn}$.

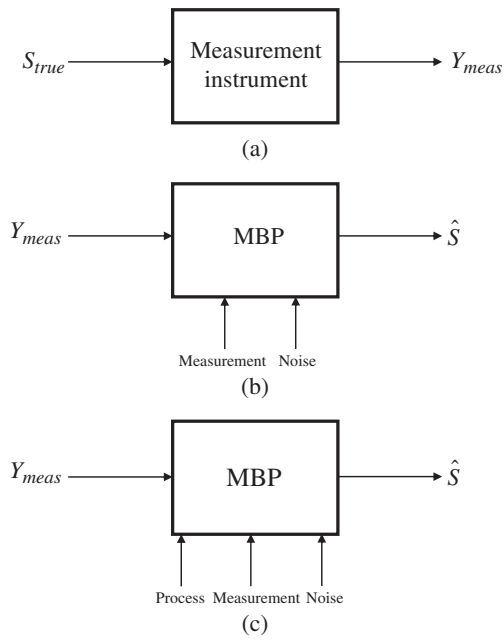


**Figure 1.9** Classes of model-based signal processors: (a) Simple measurement systems. (b) Model-based signal processing with measurement instrument modeling. (c) Model-based signal processing with measurement uncertainty and process modeling.

We can also specify the estimation error variance $\tilde{R}$ or equivalently the quality of this processor in estimating $S$. Finally, if we incorporate not only instrumentation knowledge, but also knowledge of the physical process (see Figure 1.9c), then we expect to do even better, that is, we expect the estimation error ($\tilde{S} = S_{true} - \hat{S}$) variance $\tilde{P}$ to be small (see Figure 1.8 for $\pm 2\sqrt{\tilde{R}}$ confidence limits or bounds) as we incorporate more and more knowledge into the processor, i.e.

$$\hat{S} = A(S_{true}) + W_{noise}, \quad W \sim \mathcal{N}(0, R_{ww}) \quad \text{[Process Model and Noise]}$$
$$Y_{meas} = C(S_{true}) + N_{noise}, \quad N \sim \mathcal{N}(0, R_{nn}) \quad \text{[Measurement Model and Noise]}$$

where $A(S_{true})$ is the process system model and $\mathcal{N}(0, R_{ww})$ is the process noise statistics captured by a zero-mean, Gaussian distribution with variance, $R_{ww}$.

In fact, this is the case because it can be shown that

$$\tilde{P} < \tilde{R} < \text{Instrument variance}$$

This is the basic idea in *MBSP*: "the more a priori information we can incorporate into the algorithm, the smaller the resulting error variance." Consider the following example to illustrate these ideas.

**Example 1.7** The voltage at the output of an RC circuit is to be measured using a high-impedance voltmeter shown in Figure 1.10. The measurement is contaminated with random instrumentation noise, which can be modeled by

$$e_{out} = K_e e + v$$

where

$e_{out}$ = measured voltage
$K_e$ = instrument amplification factor
$e$ = true voltage
$v$ = zero-mean random noise of variance, $R_{vv}$

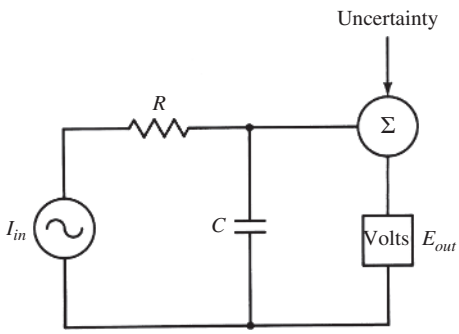


**Figure 1.10** Model-based signal processing "model" for an RC circuit.

This model corresponds to that described in Figure 1.9b. A processor is to be designed to improve the precision of the instrument. Then, as in the figure we have

- Measurement:

$$\begin{aligned} S &\to e \\ Y &\to e_{out} \\ C(\cdot) &\to K_e \\ N &\to v \\ R_{nn} &\to R_{vv} \end{aligned}$$

- and for the filter,

$$\begin{aligned} \hat{s} &\to \hat{e} \\ \tilde{R}_{ss} &\to \tilde{R}_{ee} \end{aligned}$$

The precision of the instrument can be improved even further by including a model of the process (circuit). Writing the Kirchhoff node equations we have the differential equation

$$\dot{e} = \frac{1}{C} I_{in} - \frac{e}{RC} + q$$

where

$$\begin{aligned} R &= \text{resistance} \\ C &= \text{capacitance} \\ I_{in} &= \text{excitation current} \\ q &= \text{zero-mean random noise of variance } R_{qq} \end{aligned}$$

The improved model-based processor employs both measurement and process models as in Figure 1.9c. Thus, we have

- Process:

$$\begin{aligned} \dot{s} &\to \dot{e} \\ A(\cdot) &\to -\frac{e}{RC} + \frac{1}{C} I_{in} \\ W &\to q \\ R_{ww} &\to R_{qq} \end{aligned}$$

- Measurement:

$$\begin{aligned} S &\to e \\ Y &\to e_{out} \end{aligned}$$

$$C(\cdot) \to K_e$$
$$N \to v$$
$$R_{nn} \to R_{vv}$$

- Therefore, the filter becomes,

$$\hat{s} \to \hat{e}$$
$$\tilde{P}_{ss} \to \tilde{P}_{ee}$$

- such that

$$\tilde{P}_{ee} < \tilde{R}_{ee} < R_{vv}$$

This completes the example. △△△

With this approach in mind, let us proceed to investigate a mechanical system characterized by a multichannel representation and see how it can easily be decomposed to yield decoupled subsystems available for analysis. First, we briefly present the generic linear time-invariant, multivariable, mass-damper-spring (*MCK*) mechanical system representation and illustrate its decomposition into constituent subsystems [13, 14].

Linear, continuous time, time-invariant multiple input/multiple output (*MIMO*) mechanical systems are characterized by the vector-matrix differential equations creating the *vibrational process model* in continuous time, $t$ given by

$$M\ddot{\mathbf{d}}(t) + C_d\dot{\mathbf{d}}(t) + K\mathbf{d}(t) = B_f\mathbf{f}(t) \tag{1.11}$$

where $\mathbf{d}$ is the $N_d \times 1$ displacement vector, $\mathbf{f}$ is the $N_f \times 1$ excitation force, and $M$, $C_d$, $K$ are the $N_d \times N_d$ lumped mass, damping, and spring constant matrices with $B_f$ the $N_d \times N_f$ input transmission matrix. The structure of these matrices, typically, takes the form as

$$M = \begin{bmatrix} M_1 & 0 & 0 & 0 & 0 \\ 0 & M_2 & 0 & 0 & 0 \\ \vdots & \vdots & \ddots & \vdots & \vdots \\ 0 & 0 & 0 & M_{N_d-1} & 0 \\ 0 & 0 & 0 & 0 & M_{N_d} \end{bmatrix}, \qquad C_d = \left[C_{d_{ij}}\right], \quad \text{and}$$

$$K = \begin{bmatrix} (K_1 + K_2) & -K_2 & 0 & 0 & 0 \\ -K_2 & (K_2 + K_3) & \ddots & 0 & 0 \\ 0 & \ddots & \ddots & -K_{N_d-1} & 0 \\ 0 & 0 & -K_{N_d-1} & \left(K_{N_d-1} + K_{N_d}\right) & -K_{N_d} \\ 0 & 0 & 0 & -K_{N_d} & K_{N_d} \end{bmatrix}$$

The corresponding measurement or output vector relation can be characterized by

$$\mathbf{y}(t) = \mathbf{C_a}\ddot{\mathbf{d}}(t) + \mathbf{C_v}\dot{\mathbf{d}}(t) + \mathbf{C_{dp}}\mathbf{d}(t) \tag{1.12}$$

where the constant matrices: $\mathbf{C_a}, \mathbf{C_v}, \mathbf{C_{dp}}$ are the respective acceleration, velocity, and displacement weighting matrices of appropriate dimension.

By performing a so-called modal (coordinate) transformation ($\mathbf{T}_m$) such that $\mathbf{d} = \mathbf{T}_m \times \mathbf{q}_m$ with $\mathbf{q}_m$ the modal vector. The resulting *modal model* evolves as [14]

$$\begin{aligned} &\ddot{\mathbf{q}}_m(t) + \underbrace{2\mathbf{Z\Omega}}_{\mathcal{Z}}\dot{\mathbf{q}}_m(t) + \underbrace{\mathbf{\Omega}^2}_{\mathcal{O}}\mathbf{q}_m(t) = \mathcal{B}_m\mathbf{f}_m(t) \\ &\mathbf{y}_m(t) = \mathcal{C}_m\mathbf{q}_m(t) \end{aligned} \tag{1.13}$$

where the *modal damping matrix* is $\mathcal{Z} = \text{diag}\left[\zeta_1, \ldots, \zeta_{N_d}\right]$ and the corresponding *modal frequency matrix* is $\mathbf{\Omega} = \text{diag}\left[\omega_1, \ldots, \omega_{N_d}\right]$. This representation is the "decoupled" or "decomposed" *MCK*-model that can be expressed as a set of uncoupled subsystems as

$$\begin{aligned} &\ddot{\mathbf{q}}_{m,i}(t) + 2\zeta_i\omega_i\dot{\mathbf{q}}_{m,1}(t) + \omega_i^2\mathbf{q}_{m,i}(t) = \mathbf{b}_{m,i}^T\mathbf{f}_{m,i}(t) \\ &\mathbf{y}_{m,i}(t) = \mathbf{c}_{m,i}^T\mathbf{q}_{m,i}(t), \qquad i = 1, \ldots, N_d \end{aligned} \tag{1.14}$$

Next, we investigate a simple mechanical system developed previously in [14].

**Example 1.8** Consider the simple 3-mass (spring-damper) mechanical system[1] illustrated in Figure 1.11 from [14] where $m_i = 1; k_i = 3; i = 1, \ldots, 3$ and $C_d = 0.01 \times K$. These parameters along with the input/output transmission matrices lead to the so-called "nodal model" of structural dynamics with $N_d = 3$.

$$M\ddot{\mathbf{d}}(t) + C_d\dot{\mathbf{d}}(t) + K\mathbf{d}(t) = B_f\mathbf{f}(t)$$

$$\underbrace{\begin{bmatrix} 1 & 0 & 0 \\ 0 & 1 & 0 \\ 0 & 0 & 1 \end{bmatrix}}_{\mathbf{M}}\ddot{\mathbf{d}}(t) + \underbrace{\begin{bmatrix} -0.06 & 0.03 & 0 \\ 0.03 & -0.06 & 0.03 \\ 0 & 0.03 & -0.03 \end{bmatrix}}_{\mathbf{C}_d}\dot{\mathbf{d}}(t) + \underbrace{\begin{bmatrix} -6 & 3 & 0 \\ 3 & -6 & 3 \\ 0 & 3 & -3 \end{bmatrix}}_{\mathbf{K}}\mathbf{d}(t) = \underbrace{\begin{bmatrix} 0 \\ 0 \\ 1 \end{bmatrix}}_{\mathbf{B}_f}\delta(t)$$

with the corresponding accelerometer output given by

$$y(t) = \underbrace{\begin{bmatrix} 1 \end{bmatrix}}_{\mathbf{C}_a}\ddot{\mathbf{d}}(t)$$

Exciting this system with an impulsive hammer strike yields the 3-mass response shown in Figure 1.12a along with its accompanying Fourier spectra in

1 See [14] for a detailed analysis of this mechanical system.

1.12b and descretizing with a sampling interval of $\triangle t = 0.01$ sec. This coupled *MCK* system can be decomposed by performing an eigen-decomposition of the system matrices [14]. That is, performing the modal decomposition of the *MCK* system with coordinate transformation (eigenvector matrix) from

$$\mathbf{T}_m = \begin{bmatrix} 0.5910 & 0.7370 & 0.3280 \\ -0.7370 & 0.3280 & 0.03 \\ 0.3280 & -0.5910 & 0.7370 \end{bmatrix}$$

yields the resulting modal system of Eq. (1.13) given by

$$\ddot{\mathbf{q}}(t) + 2 \times \underbrace{\begin{bmatrix} 0.0156 & 0 & 0 \\ 0 & 0.0108 & 0 \\ 0 & 0 & 0.0039 \end{bmatrix}}_{\mathbf{Z}} \times \underbrace{\begin{bmatrix} 3.1210 & 0 & 0 \\ 0 & 2.1598 & 0 \\ 0 & 0 & 0.7708 \end{bmatrix}}_{\boldsymbol{\Omega}} \dot{\mathbf{q}}(t)$$
$$+ \underbrace{\begin{bmatrix} 3.1210 & 0 & 0 \\ 0 & 2.1598 & 0 \\ 0 & 0 & 0.7708 \end{bmatrix}^2}_{\boldsymbol{\Omega}^2} \mathbf{q}(t) = \underbrace{\begin{bmatrix} 0.3280 \\ -0.5910 \\ 0.7370 \end{bmatrix}}_{\mathbf{B}_m} \delta(t)$$

with the velocity output matrix given by

$$y_m(t) = \mathbf{c}_{mv,1}^T \mathbf{q}(t) + \mathbf{c}_{mv,2}^T \dot{\mathbf{q}}(t) = \underbrace{\begin{bmatrix} 0.7370 & 0 & 0 \end{bmatrix}}_{\mathbf{c}_{mv,1}^T} \mathbf{q}(t) + \underbrace{\begin{bmatrix} 0 & 0.7370 & -0.5910 \end{bmatrix}}_{\mathbf{c}_{mv,2}^T} \dot{\mathbf{q}}(t)$$

The decomposed modal model is now available. Each of the modal subsystem responses and spectra can be obtained as illustrated by the corresponding impulse responses and spectra shown in Figure 1.11. Comparing the individual spectra with the composite spectra consisting of the set of frequencies $\{f_i = 0.497, 0.343, 0.123\,\text{Hz}\}$ have been extracted by the modal decomposition. This completes the model-based decomposition example.

△△△

Before we depart from this chapter, let us define the notation to be used throughout the text and then summarize the chapter.

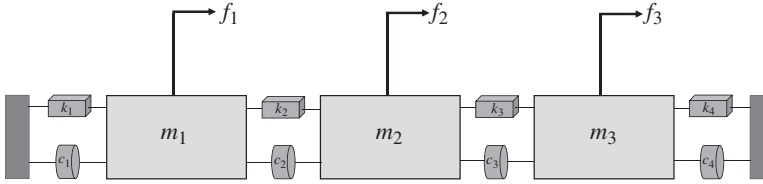


**Figure 1.11** The 3-mass mechanical system under investigation.

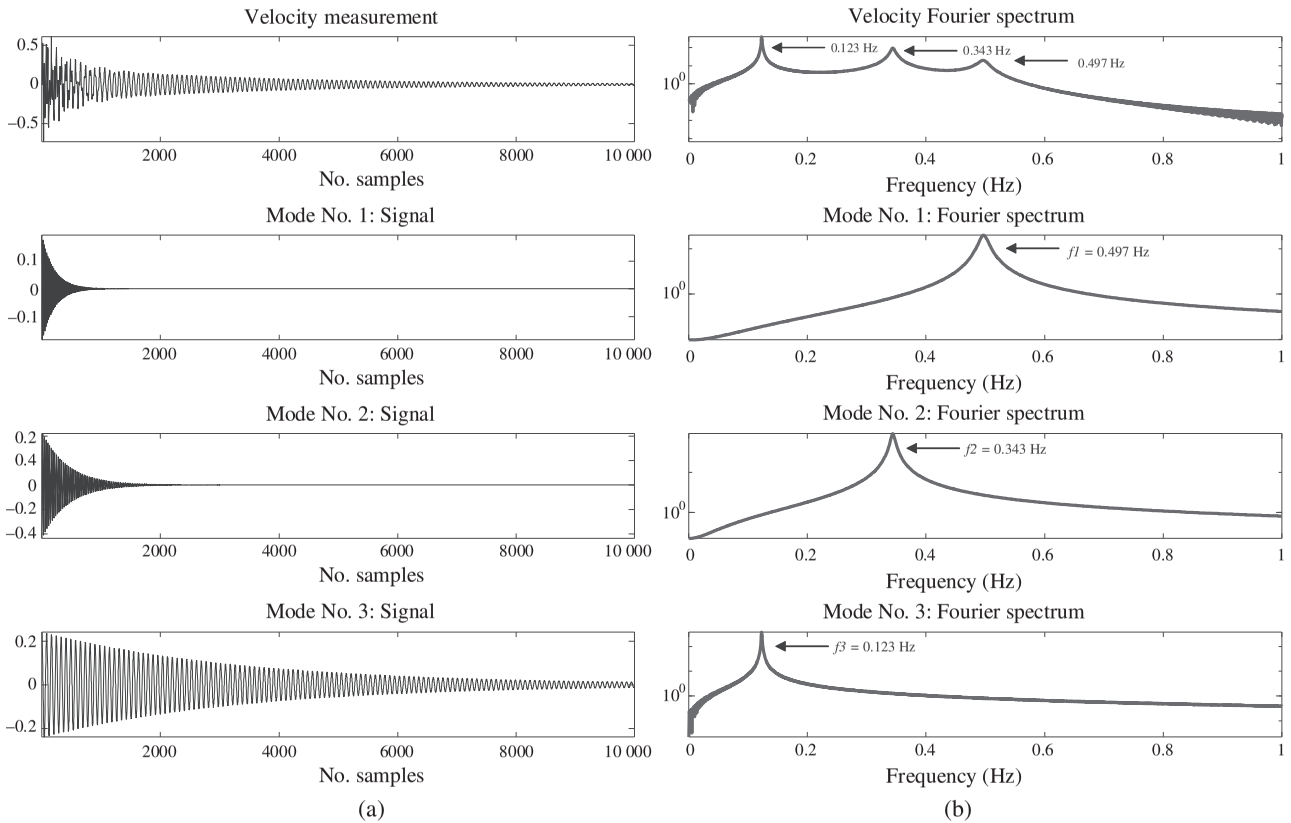


**Figure 1.12** Decomposition of 3-mass mechanical system. (a) Composite channel impulse responses and individual modal responses. (b) Fourier transforms of composite channel responses with spectral peaks at 0.497, 0.343, 0.123 Hz and individual constituent Fourier spectra obtained from system modal decomposition.

## 1.5 Notation and Terminology

The notation used throughout this text is standard in the literature. Where necessary, vectors are represented by boldface, lowercase, $\mathbf{x}$, and matrices by boldface, uppercase, $\mathbf{A}$. The *adjoint* of the matrix $\mathbf{A}$ is annotated as $\text{adj}(\mathbf{A})$ and its corresponding *determinant* by $\det(\mathbf{A})$. We define the notation $N$ to be a shorthand way of writing $1, 2, \ldots, N$. It will be used in matrices, $A(N)$ to mean there are $N$-columns of $A$. We also use the equivalent *MATLAB* notation $(1 : N)$. We denote the real part of a signal by Re and its imaginary part by Im. As mentioned previously, estimators are annotated by the caret, such as $\hat{x}$. We also define partial derivatives at the component level by $\frac{\partial}{\partial \theta_i}$, the $N_\theta$-gradient vector by $\nabla_\theta$ and higher order partials by $\nabla^2_\theta$.

The most difficult notational problem will be with the "time" indices. Since this text is predominantly discrete-time, we will use the usual time symbol, $t$ to mean a discrete-time index, i.e. $t \in \mathcal{I}$ for $\mathcal{I}$ the set of integers. However, and hopefully not too confusing, $t$ will also be used for continuous-time, i.e. $t \in \mathcal{R}$ for $\mathcal{R}$ the set of real numbers denoting the continuum. When used as a continuous-time variable, $t \in \mathcal{R}$ it will be represented as a subscript to distinguish it, i.e. $x_{\mathbf{t}}$. This approach of choosing $t \in \mathcal{I}$ primarily follows the system identification literature for the ease of recognizing discrete-time variable in transform relations (e.g. *DFT*). The rule-of-thumb is therefore to "interpret $t$ as a discrete-time index unless noted by a subscript as continuous in the text." With this in mind, we will define a variety of discrete estimator notations as $\hat{x}(t|t-1)$ to mean the estimate at time (discrete) $t$ based upon all of the previous data up to $t-1$. We will define these symbols prior to their use with the text to assure no misunderstanding of their meaning.

With a slight abuse of notation, we will use the terminology *distribution* of $X$, $\Pr(X)$ in general, so as not to have to differentiate between density for continuous random variables or processes and mass for discrete variates. It will be obvious from the context which is meant. In some cases, we will be required to make the distinction between cumulative distribution function (*CDF*) and density (*PDF*) or mass (*PMF*) functions. Here we use the uppercase notation, $\mathrm{P}_X(x)$ for the *CDF* and lower case $\mathrm{p}_X(x)$ for the *PDF* or *PMF*.

Subsequently, we will also need to express a discrete *PMF* as a continuous *PDF* using impulse or delta functions as "samplers" much the same as in signal processing when we assume there exists an impulse sampler that leads to the well-known Nyquist sampling theorem [1]. Thus, corresponding to a discrete *PMF*, we can define a continuous *PDF* through the concept of an *impulse sampler*, that is, given a discrete *PMF* defined by

$$\mathrm{p}_X(x) \approx \mathrm{p}(X = x_i) = \sum_i p_i \; \delta(x - x_i) \tag{1.15}$$

then we define the *equivalent continuous PDF* as $\mathrm{p}_X(x)$. Moments follow from the usual definitions associated with a continuous *PDF*, for instance, consider the definition of the expectation or mean. Substituting the equivalent *PDF* and utilizing the sifting property of the impulse function gives

$$E\{x\} = \int_{-\infty}^{\infty} x\ \mathrm{p}_X(x)\ dx = \int_{-\infty}^{\infty} x \left( \sum_i p_i \delta(x - x_i) \right) dx = \sum_i x_i\ p_i \tag{1.16}$$

which is precisely the mean of the discrete *PMF* (see Appendix A for more details).

Also, as mentioned, we will use the symbol $\sim$ to mean "distributed according to" as in $x \sim \mathcal{N}(m, v)$ defining the random variable $x$ as Gaussian distributed with mean $m$ and variance $v$. We may also use the extended notation: $\mathcal{N}(x : m, v)$ to include the random variable $x$ as well. When *sampling* we use the *nonconventional* right arrow "action" notation $\longrightarrow$ to mean "draw a sample from" a particular distribution such as $x_i \rightarrow \Pr(x)$–this again will be clear from the context. When *resampling*, that is, replacing samples with new ones we use the "block" right arrow such as $x_j \Rightarrow x_i$ meaning new sample $x_j$ replaces current sample $x_i$. In a discrete (finite) probabilistic representation, we define a purely discrete variate as $x_k(t) := \Pr(x(t) = \mathcal{X}_k)$ meaning that $x$ can only take on values (integers) $k$ from a known set $\mathcal{X} = \{\mathcal{X}_1, \ldots, \mathcal{X}_k, \ldots, \mathcal{X}_N\}$ at time $t$. We also use the symbol $\triangle\triangle\triangle$ to mark the end of an example.

We define two projection operators: (i) orthogonal; and (ii) oblique or parallel. The *orthogonal projection operator* "projects" $\bullet$ onto $\mathcal{Y}$ as $\mathcal{P}_{\bullet|\mathcal{Y}}$ or its complement $\mathcal{P}^{\perp}_{\bullet|\mathcal{Y}}$, while the *oblique projection operator* "projects" $\bullet$ onto $\mathcal{Y}$ "along" $\mathcal{Z}$ as $\mathcal{P}^{\parallel}_{\bullet|\mathcal{Y}\circ\mathcal{Z}}$. For instance, orthogonally projecting the vector $\mathbf{x}$, we have $\mathcal{P}_{\mathbf{x}|\mathcal{Y}}$ or $\mathcal{P}^{\perp}_{\mathbf{x}|\mathcal{Y}}$, while obliquely projecting $\mathbf{x}$ along $\mathcal{Z}$ is $\mathcal{P}_{\mathbf{x}|\mathcal{Y}\circ\mathcal{Z}}$ (see Appendix B). The matrix projection operator evolves from decompositions such as the LQ-decomposition (see Appendix C) where the operator is given in terms of its orthonormal bases as $\mathcal{P} = Q \times Q'$.

## 1.6 Summary

In this chapter, we have introduced the concept of decomposition starting with the simple notion of transforming a signal into an alternate domain to analyze and extract the desired information. With this in mind, data-based decomposition was investigated with the primary idea that signal/measurement data could be used to construct a variety of formats leading to the usual vector-matrix form that dominates the signal processing techniques. Finally, *MBSP* was introduced based on the idea of incorporating more and more any available a priori information into the processing scheme leading to the model-based decomposition approach. A simple 3-mass mechanical system was analyzed and followed throughout the

chapter demonstrating how the various approaches can be applied to achieve a decomposition of the composite signal into constituent components. Various signals were classified as deterministic or random. When the signal is random the resulting processors are called estimation filters or estimators. A procedure was defined (estimation procedure) leading to a formal processing approach to extract information based on prior knowledge of the composition which will be used throughout this text. After a couple of examples motivating the concept of *MBSP*, a more formal discussion followed with *RC* and *MCK* circuit examples completing the chapter. Finally, the notation utilized throughout the text was discussed completing this introductory chapter.

## MATLAB® Notes

*MATLAB*® is command-oriented vector-matrix package with a simple yet effective command language featuring a wide variety of embedded *C* language constructs making it ideal for signal processing and graphics. All of the algorithms we have applied to the examples and problems in this text are *MATLAB*-based in solutions ranging from simple simulations to complex applications. We will develop these notes primarily as a summary to point out to the reader many of the existing commands that already perform the signal processing operations discussed in the presented chapter and throughout the text.

## References


1 Candy, J. (2006). *Model-Based Signal Processing*. Hoboken, NJ: Wiley/IEEE Press.
2 Hayes, M. (1996). *Statistical Digital Signal Processing and Modeling*. New York: Wiley.
3 Golub, G. and Van Loan, C. (1984). *Matrix Computations*. Baltimore, MD: Johns Hopkins University Press.
4 Rainieri, C. and Fabbrocino, G. (2014). *Operational Modal Analysis of Civil Engineering Structures*. New York: Springer.
5 Reynders, E. (2012). System identification methods for (operational) modal analysis: review and comparison. *Arch. Comput. Meth. Eng.* 19 (1): 51–124.
6 Schmidt, R. (1986). Multiple emitter location and signal processing estimation. *IEEE Trans. Antennas Propg.* 34 (3): 276–280.
7 Fink, M. (1997). Time reversed acoustics. *Phys. Today* 50: 34–40.
8 Johnson, D. and Mersereau, R. (1993). *Array Signal Processing*. New Jersey: Prentice-Hall.

**9** Nielson, R. (1995). *Sonar Signal Processing*. New Jersey: Prentice-Hall.
**10** Candy, J. (2008). Signal processing in acoustics: science or science fiction? *Acoust. Today* 4 (3): 6–15.
**11** Candy, J. (1986). *Signal Processing: The Model-Based Approach*. New York: McGraw-Hill.
**12** Jazwinski, A. (1970). *Stochastic Processes and Filtering Theory*. New York: Academic Press.
**13** Meirovitch, L. (1990). *Dynamics and Control of Structures*. New York: Wiley.
**14** Gawronski, W. (2004). *Advanced Structural Dynamics and Active Control of Structures*. New York: Springer.

## Problems

**1.1** A one-story structure is monitored for potential damage after being subjected to an earthquake. Cars and trucks passing by provide the excitation modeled as random noise. The displacement of the structure is acquired by placing an accelerometer at a critical location sensitive to these vibrations. The accelerometer has inherent inaccuracies which is modeled as

$$y = K_b x + n$$

with $y$, $x$, $n$ the measured and actual displacement and white measurement noise of variance $R_{nn}$ and $K_b$ the instrument gain. The dynamics of the vibrating structure is modeled by a simple mass-spring-damper ($MCK$) system.

(a) Construct and identify the measurement model of this system identifying each of its components.
(b) Construct and identify the process model and model-based estimator for this problem.
(c) What is the variance associated with each modeling phase: measurement, process, and noise?

**1.2** We are asked to estimate the displacement of large vehicles (semi-trailers) when parked on the shoulder of a freeway and subjected to wind gusts created by passing vehicles. We measure the displacement of the vehicle by placing an accelerometer on the trailer. The accelerometer has inherent inaccuracies which is modeled as

$$y = K_a x + n$$

with $y$, $x$, $n$ the measured and actual displacement and white measurement noise of variance $R_{nn}$ and $K_a$ the instrument gain. The dynamics of the vehicle can be modeled by a simple mass-spring-damper.

(a) Construct and identify the measurement model of this system.
(b) Construct and identify the process model and model-based estimator for this problem.

**1.3** Think of measuring the temperature of a liquid in a breaker heated by a burner. Suppose we use a thermometer immersed in the liquid and periodically observe the temperature and record it.
(a) Construct a measurement model assuming that the thermometer is linearly related to the temperature, that is, $y(t) = k\triangle T(t)$. Also model the uncertainty of the visual measurement as a random sequence $v(t)$ with variance $R_{vv}$.
(b) Suppose we model the heat transferred to the liquid from the burner as

$$Q(t) = CA\triangle T(t)$$

where $C$ is the coefficient of thermal conductivity, $A$ is the cross-sectional area, and $\triangle T(t)$ is the temperature gradient with assumed random uncertainty $w(t)$ and variance $R_{ww}$. Using this process model and the models developed above, identify the model-based processor representation.

**1.4** We are given an *RLC* series circuit driven by a noisy voltage source $V_{in}(t)$ and we use a measurement instrument that linearly amplifies by $K$ and measures the corresponding output voltage. We know that the input voltage is contaminated by an additive noise source, $w(t)$ with covariance, $R_{ww}$ and the measured output voltage is similarly contaminated with noise source, $v(t)$ with $R_{vv}$.
(a) Determine the model for the measured output voltage, $V_{out}(t)$ (measurement model).
(b) Determine a model for the circuit (process model).
(c) Identify the general model-based processor structures depicted in Figure 1.9. In each scheme, specify the models for the process, measurement, and noise.

**1.5** A communications satellite is placed into orbit and must be maneuvered using thrusters to orientate its antennas. Restricting the problem to the single axis perpendicular to the page, the equations of motion are

$$J\frac{d^2\theta}{dt^2} = T_c + T_d$$

where $J$ is the moment of inertia of the satellite about its center of mass, $T_c$ is the thruster control torque, $T_d$ is the disturbance torque, and $\theta$ is the angle

of the satellite axis with respect to the inertial reference (no angular acceleration) $A$. Develop signal and noise models for this problem and identify each model-based processor component.

**1.6** Consider a process described by a set of linear differential equations

$$\frac{d^2c}{dt^2} + \frac{dc}{dt} + c = Km$$

The process is to be controlled by a proportional-integral-derivative (PID) control law governed by the equation

$$m = K_p\left(e + \frac{1}{T_i}\int edt + T_d\frac{de}{dt}\right)$$

and the controller reference signal $r$ is given by

$$r = e + c$$

Suppose the reference is subjected to a disturbance signal and the measurement sensor, which is contaminated with additive noise, measures the "square" of the output. Develop the model-based signal and noise models for this problem as in Figure 1.9.

**1.7** The elevation of a tracking telescope is controlled by a DC motor. The telescope has a moment of inertia $J$ and damping $B$ due to friction, the equation of motion is given by

$$J\frac{d^2\theta}{dt^2} + B\frac{d\theta}{dt} = T_m + T_d$$

where $T_m$ and $T_d$ are the motor and disturbance torques and $\theta$ is the elevation angle. Assume a sensor transforms the telescope elevation into a proportional voltage that is contaminated with noise. Develop the signal and noise models for the telescope and identify all of the model-based processor components.